Metal–Support Interactions

International Edition: DOI: 10.1002/anie.201410697
German Edition: DOI: 10.1002/ange.201410697

In Situ and Theoretical Studies for the Dissociation of Water on an Active Ni/CeO_2 Catalyst: Importance of Strong Metal–Support Interactions for the Cleavage of O–H Bonds**

Javier Carrasco, David López-Durán, Zongyuan Liu, Tomáš Duchoň, Jaime Evans, Sanjaya D. Senanayake, Ethan J. Crumlin, Vladimir Matolín, José A. Rodríguez, and M. Verónica Ganduglia-Pirovano**

Abstract: *Water dissociation is crucial in many catalytic reactions on oxide-supported transition-metal catalysts. Supported by experimental and density-functional theory results, the effect of the support on O–H bond cleavage activity is elucidated for nickel/ceria systems. Ambient-pressure O1s photoemission spectra at low Ni loadings on CeO_2(111) reveal a substantially larger amount of OH groups as compared to the bare support. Computed activation energy barriers for water dissociation show an enhanced reactivity of Ni adatoms on CeO_2(111) compared with pyramidal Ni_4 particles with one Ni atom not in contact with the support, and extended Ni(111) surfaces. At the origin of this support effect is the ability of ceria to stabilize oxidized Ni^{2+} species by accommodating electrons in localized f-states. The fast dissociation of water on Ni/CeO_2 has a dramatic effect on the activity and stability of this system as a catalyst for the water-gas shift and ethanol steam reforming reactions.*

Water dissociation at surfaces is important in corrosion, solar energy conversion processes that split water, and in numerous heterogeneous catalytic reactions on oxide-supported transition-metal catalysts.[1–3] Dissociative chemisorption of H_2O on a catalyst surface, an apparently simple process, can be an important reaction step, affecting the performance of many catalytic processes.[3] Therefore, being able to control the ability of a catalyst to dissociate water is highly desirable. However, this is a challenging task. For example, Hundt et al.[4] have recently shown how complex water dissociation can be at the atomic level even on a relatively simple system, namely a well-defined Ni(111) metal surface. For oxide-supported metal nanoparticles, our knowledge of the water dissociation process remains in its infancy. This is because of the difficulties associated with the study of metal/oxide catalysts.[3] On these systems, the dissociation of water can be affected by the metal particle size, the nature of the oxide support, and the strength of the metal–support interactions. Shedding light into such structure–reactivity relationships has the potential for boosting the catalytic performance of this class of metal oxide materials. Herein, using a combination of ambient-pressure X-ray photoelectron spectroscopy (AP-XPS) and density-functional theory (DFT) calculations, we investigate the dissociation of water on a model Ni/CeO_2(111) catalyst. Strong electronic perturbations induced by Ni–CeO_2 interactions lead to an unexpectedly low activation barrier for water dissociation, a phenomenon that can be used to enhance the activity and selectivity of catalytic processes.

Previous studies have shown that the Ni/CeO_2 system has outstanding catalytic activity and selectivity for both the water-gas shift (WGS, $CO + H_2O \rightarrow H_2 + CO_2$) and the ethanol steam reforming reactions (ESR, $C_2H_5OH + 3H_2O \rightarrow 6H_2 + 2CO_2$).[5–8] The behavior of ceria-supported nickel is quite different from that of bulk nickel, a system that is very good for CO methanation and undergoes rapid deactivation by coke deposition during the steam reforming of ethanol.[5,7,8] The results of core and valence photoemission

[*] Dr. J. Carrasco, Dr. D. López-Durán,[+] Dr. M. V. Ganduglia-Pirovano
Instituto de Catálisis y Petroleoquímica, CSIC
C/Marie Curie 2, 28049 Madrid (Spain)
E-mail: vgp@icp.csic.es
Dr. Z. Liu, Dr. S. D. Senanayake, Dr. J. A. Rodríguez
Chemistry Department, Brookhaven National Laboratory
Upton, NY 11973 (USA)
E-mail: rodrigez@bnl.gov
Dr. T. Duchoň, Prof. Dr. V. Matolín
Faculty of Mathematics and Physics, Charles University
V Holešovičkách 2, Praha 8 (Czech Republic)
Dr. J. Evans
Facultad de Ciencias, Universidad Central de Venezuela
Caracas 1020A (Venezuela)
Dr. E. J. Crumlin
Advanced Light Source, Lawrence Berkeley National Laboratory
Berkeley, CA 94720 (USA)
Dr. J. Carrasco, Dr. D. López-Durán[+]
CIC Energigune, Albert Einstein 48, 01510 Miñano, Álava (Spain)
Dr. Z. Liu, Dr. J. A. Rodríguez
Dept. of Chem., SUNY, Stony Brook, NY 11749 (USA)
[+] Present address: Departamento de Química Analítica
Química Física e Ingeniería Química
Universidad de Alcalá, 28871 Alcalá de Henares, Madrid (Spain)

[**] This work has been supported by the MINECO-Spain (CTQ2012-32928), the Ministry of Education of the Czech Republic (LH11017), and the U.S. Department of Energy (DE-AC02-98CH10886, DE-AC02-05CH11231). J.C. acknowledges support by the Ramón y Cajal Fellowship, the Marie Curie Career Integration Grant FP7-PEOPLE-2011-CIG: Project NanoWGS and The Royal Society through the Newton Alumnus scheme. The COST action CM1104 is gratefully acknowledged. Computer time provided by the SGAI-CSIC, CESGA, BIFI-ZCAM, IFCA, and the BSC is acknowledged.

Supporting information for this article is available on the WWW under http://dx.doi.org/10.1002/anie.201410697.

(Supporting Information, Figure S1 and S2) plus DFT calculations (Figure S3) indicate that Ni atoms in contact with $CeO_2(111)$ are electronically perturbed.[7–9] They exhibit a very low density-of-states near the Fermi level (Figure S2 and S3) and a +2 oxidation state (triplet $3d^8$ state).[7,8] In Ni $2p_{3/2}$ XPS spectra, they display the line-shape and binding energy expected for Ni^{2+} (Figure S1), with a shift in the main peak of about 2 eV with respect to that of Ni^0.[10] At $\Theta_{Ni} < 0.2$ ML (monolayers), these Ni^{2+} species are not able to catalyze CO methanation but exhibit a high activity for the WGS reaction (Figure S4).[6,7] A fundamental question remains: How fast is the dissociation of water on a Ni/CeO_2 surface? Ni(111) is not very active for the $H_2O \rightarrow OH + H$ process.[1,4]

Using AP-XPS, we investigated the adsorption of water on $CeO_2(111)$ and on a $Ni/CeO_2(111)$ surface with a small coverage of electronically perturbed Ni ($\Theta_{Ni} \approx 0.15$ ML). The background pressure of water and the temperature of the surface had a strong influence on the type and amount of species adsorbed on $CeO_2(111)$ (Supporting Information, Figure S5) and $Ni/CeO_2(111)$ (Figure 1). Under ultrahigh vacuum conditions ($p_{H_2O} < 10^{-7}$ Torr), we did not observe adsorption of water at room temperature. However, water adsorption was seen when the samples were under water pressures above 1×10^{-4} Torr. Part of the chemisorbed water molecules dissociated to produce OH groups on the surface. At temperatures of 500 and 700 K, even under a background water pressure of 200 mTorr, there was almost no chemisorbed water on the surfaces and the concentration of adsorbed OH was also smaller than at 300 K.

Figure 2 shows the curve-fitting of the O 1s XPS spectra collected for $CeO_2(111)$ and $Ni/CeO_2(111)$ under a water pressure of 200 mTorr at 300 and 500 K. At 300 K, peaks can be clearly seen for gaseous H_2O, chemisorbed H_2O, adsorbed OH groups, and O from the lattice of ceria. After curve-fitting the O 1s spectra, the amount of water and OH groups present on the surface at 300 K is larger for $Ni/CeO_2(111)$ than for $CeO_2(111)$. For example, the OH coverage increases from 0.78 ML on $CeO_2(111)$ to 0.90 ML on $Ni/CeO_2(111)$. The enhancement in the signals for H_2O and OH is small (10–25%), but it is consistent with the fact that we only had a small amount of Ni supported on ceria ($\Theta_{Ni} \approx 0.15$ ML). Annealing from 300 to 500 K led to the almost disappearance of the signal for chemisorbed H_2O and a substantial fraction of the adsorbed OH groups were also removed from both surfaces. However, as shown in Figure 2, the amount of OH present on $Ni/CeO_2(111)$ at 500 K, 0.37 ML, was about a factor of two larger than on $CeO_2(111)$, 0.20 ML. This larger coverage of OH should facilitate the WGS and ESR reactions. The OH groups can easily react with CO and CH_x fragments to yield CO_2 and H_2.[5–7]

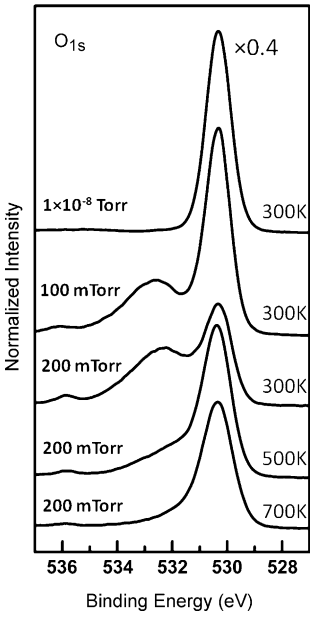

Figure 1. O 1s XPS spectra for a $Ni/CeO_2(111)$ surface (Θ_{Ni} ca. 0.15 ML) under different background pressures of water (1×10^{-8} Torr, 100, and 200 mTorr) at 300 K, and during annealing from 300 to 500 K under 200 mTorr of water.

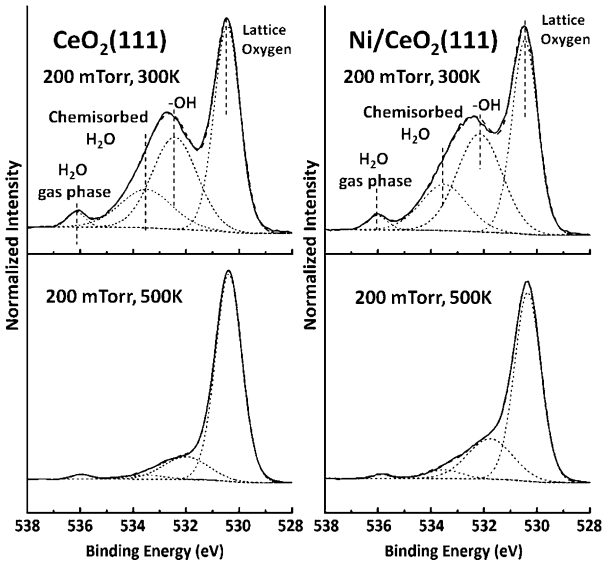

Figure 2. O 1s XPS spectra for $CeO_2(111)$ and $Ni/CeO_2(111)$ under 200 mTorr of water at 300 and 500 K. The coverage of Ni in $Ni/CeO_2(111)$ was about 0.15 ML.

We performed DFT calculations to gain insight into the energetics and mechanism for the dissociation of water on $Ni/CeO_2(111)$. Results of scanning tunneling microscopy (STM) indicate that the ceria substrates used in this study exhibited (111) terraces and a large number of defects and imperfections. These defects and imperfections affect the growth mode of Ni on the ceria.[9] At small coverages (< 0.2 ML), Ni is present on the $CeO_2(111)$ substrate as adatoms and small clusters or particles that can have two-dimensional (single layer) or three-dimensional (more than one layer) shapes.[9] All these nickel species exhibit an oxidation state close to +2 in XPS and UPS measurements (Supporting Information, Figures S1 and S2).[5] Ni interacts strongly with the ceria substrate and upon heating penetrates into the oxide support.[7,11] Solid solutions of the $Ce_{1-x}Ni_xO_{2-y}$ ($x < 0.2$) type can be formed.[5,6] In a previous study, the geometry and electronic structure of isolated Ni atoms (Ni_1) and Ni_4 clusters supported on the $CeO_2(111)$ surface have been studied (Supporting Information, Figure S3).[8] In the case of the

$Ni_1/CeO_2(111)$ system, nickel exhibited an oxidation state of +2 and can be taken as a model for individual adatoms on the ceria surface and for Ni atoms in supported particles that exhibit a high oxidation state in photoemission and XPS studies.[7,9] For the $Ni_4/CeO_2(111)$ system, the most stable nickel cluster has a pyramidal configuration with three nickel atoms touching the oxide support and one away from the surface (a rombohedral quasi-planar configuration is only about 0.2 eV less stable; Supporting Information, Figure S3 and Table S1).[8] The average oxidation state of nickel (ca. +0.5) in $Ni_4/CeO_2(111)$ was smaller than on $Ni_1/CeO_2(111)$.[8] For pyramidal Ni_4 (Ni_4-pyr), Bader charges reflect that the three base atoms in direct contact with the ceria surface are positively charged whereas the one at the top is essentially neutral (Supporting Information, Table S1). Thus, there is a rapid weakening in the strength of the metal–oxide interactions when the Ni moves away from the oxide support. Since a $Ni/CeO_2(111)$ ($\Theta_{Ni} \approx 0.15$ ML) surface contains individual Ni atoms and small clusters or particles,[7,9] the modeling of the adsorption of water can be a complex task. Here, we apply the spin-polarized DFT+U approach as implemented in the Vienna ab initio simulation package (VASP)[12] to investigate the adsorption and dissociation of H_2O on the $Ni_n/CeO_2(111)$ ($n=1$ and 4) systems as well as on non-reduced and reduced $CeO_{2-x}(111)$ supports, plus the extended Ni(111) surface. Thus, we will compare the reaction of water on a system that has strong electronic perturbations, $Ni_1/CeO_2(111)$, on a system with moderate electronic perturbations where Ni is moving away from the oxide support, Ni_4-pyr/$CeO_2(111)$, and on a system in a pure metallic state, Ni(111). The comparison will enable us to identify how the electronic perturbations on Ni affect the reactivity of this metal towards water.

First we review and discuss water adsorption on the bare $CeO_2(111)$ substrate. Molecular water adsorption (Figure 3a) is about 0.4 eV energetically more favorable than complete dissociative adsorption (Figure 3c).[13–16] Nevertheless, the molecular state can easily coexist with a OH-pair-like configuration (Figure 3b), since these two configurations are separated by a small energy barrier barrier (≤ 0.15 eV).[14,16–18] In contrast, the presence of O vacancies on the surface significantly enhances water dissociation (Figure 3e) over molecular adsorption (Figure 3d).[15,16] This process is indeed quite exothermic by 1.15 eV and it is effectively barrierless[16] (Figure 4), resulting in the water OH group readily healing the O vacancy and the remaining H atom being adsorbed on top of a nearest neighbor surface O atom. However, from a catalytic viewpoint, the OH groups formed in this way are expected to be less-reactive than those on top of a regular $CeO_2(111)$ surface. When the calculated reaction energies for water dissociation in Figure 3 (−0.6 to −1.9 eV) are compared with the stability seen for the OH groups on $CeO_2(111)$ in the AP-XPS spectra of Figure 2, it can be concluded that the surface defects present in the ceria films used for the experiments probably played an important role in the binding and dissociation of water on the ceria support.

On the $Ni_1/CeO_2(111)$ system, water adsorbs exothermically ($\Delta E = -0.67$ eV) on top of a Ce^{4+} site far away from the

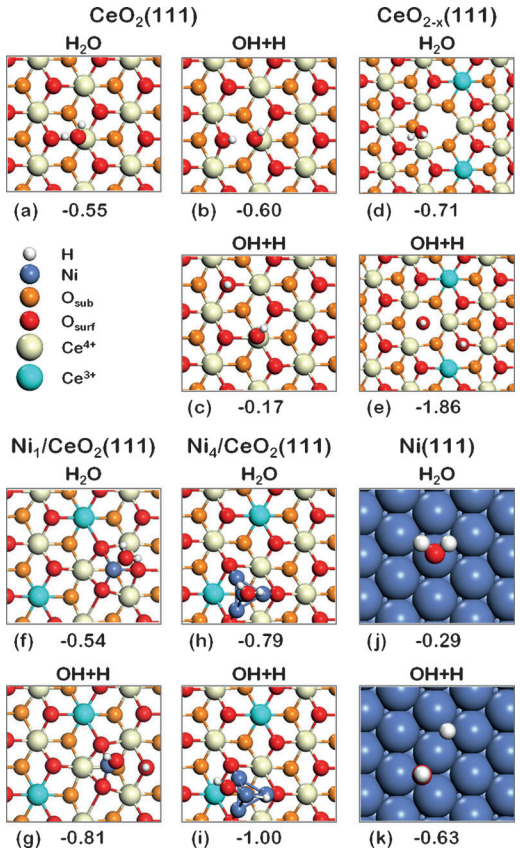

Figure 3. Atomic structure of H_2O adsorbed on: a)–c) CeO_2 (111), d),e) $CeO_{2-x}(111)$, f),g) $Ni_1/CeO_2(111)$, h),i) $Ni_4/CeO_2(111)$, and j),k) Ni(111). Adsorption energies are given with respect to gas-phase molecules in eV.

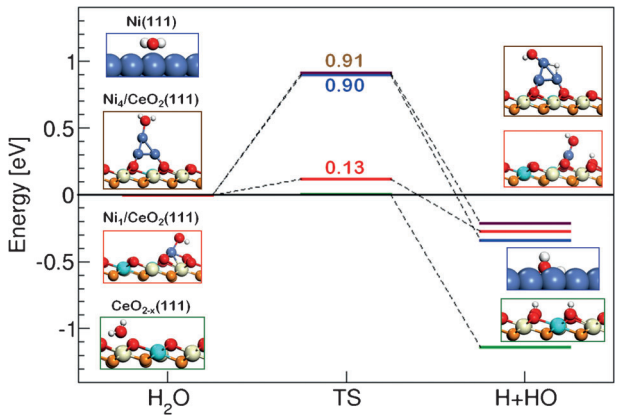

Figure 4. Reaction energy profile for H_2O dissociation on the CeO_{2-x}(111), $Ni_1/CeO_2(111)$, $Ni_4/CeO_2(111)$, and Ni(111) surfaces. The side views of the optimized initial and final state structures in Figure 3 are included.

Ni adatom (Supporting Information, Figure S6a). Adsorption on top of a Ni^{2+} site is less stable (Figure 3f), but only by 0.13 eV. The H_2O dissociation (Figure 3g) is favored by 0.27 eV and the process is hindered by a very small energy barrier of 0.13 eV (Figure 4). Note that if the proton is moved to a next-nearest surface O to the Ni–OH species (close to the

upper Ce^{3+} in Figure 3g), the system is further stabilized by 0.18 eV (Supporting Information, Figure S6c); however, the energy barrier for H diffusion on the ceria support is likely to be large (ca. 1.8 eV).[19] Therefore, as O vacancies at the $CeO_2(111)$ surface, Ni adatoms are effective active sites for H_2O dissociation. However, the OH groups formed on the $Ni_1/CeO_2(111)$ system upon dissociation, remain moderately bound to the Ni adatom and can therefore participate in the subsequent reaction steps (Figure 4). On the Ni_4-pyr/CeO_2-(111) system, the atom in the tip of the Ni_4 pyramid is not in direct contact with the oxide substrate and has a reactivity that is not very different from that of the atoms in Ni(111). On the $Ni_4/CeO_2(111)$ and Ni(111) surfaces, H_2O dissociation is exothermic by 0.21 (Figure 3h,i) and 0.34 eV (Figure 3j,k), respectively. Similar to the Ni_1 species, for the $Ni_4/CeO_2(111)$ system, the further separation of OH and H chemisorbed species leads to an stabilization of the system (Supporting Information, Figure S7b and S7c).

A comparison of the energy barriers for H_2O dissociation in Figure 4 (see the Supporting Information, Figure S8, for the transition-state structures) for Ni_4-pyr/$CeO_2(111)$ and Ni(111) points to the unique catalytic activity for H_2O dissociation of ceria supported Ni when this is present in the form of Ni^{2+}cations in contact with the ceria support. In particular, the energy barrier for the dissociation of a water molecule adsorbed on top of a supported Ni_4-pyr cluster is 0.91 eV (Figure 4), which is very close to the value of 0.90 eV found for Ni(111), in agreement with a previous report.[20] This result reveals that an atom present in a small Ni_4 cluster already resembles the reactivity of extended surfaces when it is not in contact with the oxide substrate. Thus, Ni^{2+} sites (generated by strong metal–support interactions) are essential for the fast dissociation of water. XPS and UPS indicate that they exists after depositing very small coverages of Ni on $CeO_2(111)$ (Supporting Information, Figures S1 and S2). In STM images,[9] they may correspond to individual Ni adatoms or to atoms in the corner of Ni particles that are in direct contact with defects of the ceria substrate. Ni^{2+} sites also can be generated by the formation of $Ce_{1-x}Ni_xO_{2-y}$ solid solutions.[5,6,11]

The ability of Ni^{2+} species supported on CeO_2 to cleave O–H bonds is not limited to the water molecule and it may be applicable to other compounds which also possess an acidic H. To this end we have investigated the dissociation of CH_3OH as a prototype of alcohols. The dissociative adsorption of methanol to form methoxy and a hydrogen adatom on $Ni_1/CeO_2(111)$ is exothermic by 0.43 eV (Supporting Information, Figure S9) with an activation barrier of only 0.23 eV (Supporting Information, Figure S10). Thus, Ni^{2+} sites probably play an important role in the steam reforming of alcohols over Ni/CeO_2 and $Ce_{1-x}Ni_xO_{2-y}$ catalysts.[5]

The fast dissociation of water of $Ni/CeO_2(111)$ versus Ni(111) has a drastic effect in the catalytic activity and stability of Ni/CeO_2 during the WGS reaction.[6,7] Figure 5 compares turnover frequencies (TOFs) for the WGS on Ni(111) and on a $Ni/CeO_2(111)$ surface with about 0.15 ML Ni ($T = 625$ K, 20 Torr of CO and 10 Torr of H_2O). For comparison, we also include the corresponding results for a Cu(111) surface, a commonly used benchmark in studies of the WGS reaction.[21,22] The TOFs show that Ni(111) is initially more active than Cu(111), but the catalytic activity of bulk Ni decreases with time as a consequence of the deposition of carbon on the surface through the Boudouard reaction: $2CO \rightarrow C + CO_2$. Since the dissociation of water on Ni(111) is not fast, the WGS cannot compete with the Boudouard reaction and eventually the surface is deactivated by the formation of a carbon layer. A similar problem has been reported for the WGS on Pt(111).[23] In the case of Ni/$CeO_2(111)$, the presence of Ni^{2+} sites not only favors the dissociation of O–H bonds but also makes more difficult the cleavage of C–O bonds.[8] The fast dissociation of water on Ni/CeO_2 also helps to prevent coke deposition during the reforming of hydrocarbons on this material.[5–7] The generated OH groups react with CH_x fragments to yield CO_2 and H_2.[5–7] Thus, the $Ni/CeO_2(111)$ system illustrates how one can manipulate metal–support interactions to improve catalytic activity and stability, a major goal in heterogeneous catalysis.[24]

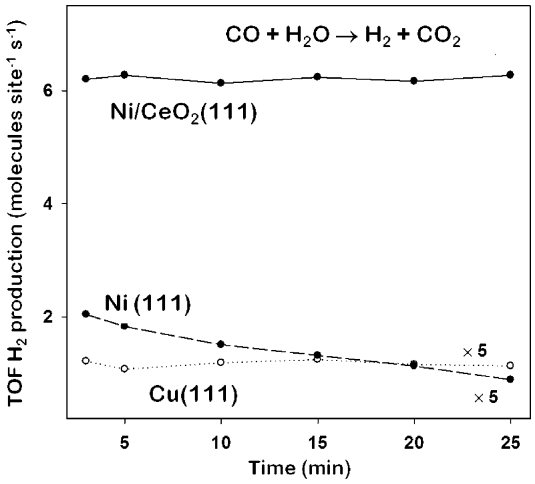

Figure 5. TOFs for the production of hydrogen through the WGS reaction on $Ni/CeO_2(111)$ ($\Theta_{Ni} \approx 0.15$ ML), Ni(111), and Cu(111). $T = 625$ K, $p_{CO} = 20$ Torr, $p_{CO} = 10$ Torr of H_2O.

Our results for $Ni/CeO_2(111)$ and recent studies for Au and Pt on different oxide substrates[25a–f] show that an oxide support can modify the electronic properties of an admetal in substantial ways. Charge polarization or a definitive change in the oxidation state can take place. This is very different from the traditional strong metal–support interaction (SMSI), which usually involved the blocking of metal active centers by oxide particles.[24,26,27] Of particular interest are single atoms of Ni (this study) and Pt[25e] dispersed on ceria, which are stable, adopt a +2 oxidation state, and exhibit chemical properties very different from those of the corresponding bulk metals.

Experimental Section

Ambient-pressure X-ray photoelectron spectroscopy (AP-XPS) studies were performed at the Advanced Light Source in Berkeley, CA, at beam-line 9.3.2. A VG-Scienta R4000 HiPP analyzer was used. The high purity of the gases was checked with an RGA and introduced by backfilling. Traps were utilized along gas lines to

prevent contamination. The O 1s region was probed with a photon energy of 700 eV and an energy resolution of 0.2–0.3 eV. The Ni/CeO_2(111) surfaces were prepared following procedures reported in the literature.[7]

The catalytic activity of the Ni(111) and Ni/CeO_2(111) samples was studied in a system which combines an ultrahigh-vacuum (UHV) chamber (base pressure ca. 5×10^{-10} Torr) and a batch reactor.[7] The sample could be transferred between the reactor and UHV chamber without exposure to air. The UHV chamber (base pressure ca. 5×10^{-10} Torr) was equipped with instrumentation for X-ray and ultraviolet photoelectron spectroscopies (XPS and UPS), low-energy electron diffraction (LEED), ion scattering spectroscopy (ISS), and temperature-programmed desorption (TPD). The amount of molecules produced in the catalytic tests was normalized by the active area exposed by the sample. Turnover frequencies (TOFs) for the Ni/CeO_2(111) ($\Theta_{Ni}\approx0.15$ ML) sample were estimated assuming that all the Ni atoms deposited on ceria participated in the catalytic reaction.

The spin-polarized calculations were performed using the DFT-(PBE) + U approach.[12] A value of 4.5 eV was used for the Hubbard U-like term. The projector augmented wave method (PAW) was used at a plane-wave cutoff of 415 eV to decouple the core from valence electrons. The C (2s, 2p), O (2s, 2p), Ni (3p, 3d, 4s), and Ce (4f, 5s, 5p, 5d, 6s) electrons were treated as valence states.

The CeO_2(111), CeO_{2-x}(111), Ni_1/CeO_2(111), Ni_4/CeO_2(111), and Ni(111) surfaces were modeled by (3 × 3) unit cells. The first four contained nine (that is, three O-Ce-O trilayers) and the last six atomics layers, respectively, separated by at least 13 Å of vacuum. The atomic geometry and electronic structure of the reduced CeO_{2-x}(111) surface with one surface defect, and those of ceria-supported Ni clusters, corresponded to those previously obtained.[8,28] Monkhorst-Pack grids with (2 × 2 × 1) and (4 × 4 × 1) k-point sampling were used for the ceria-based systems and Ni(111) surface, respectively. All of the atoms in the three bottom layers were fixed at their optimized bulk-truncated positions during geometry optimization, whereas the rest of the atoms were allowed to fully relax.

To locate the transition state structures (TS) we employed the climbing image nudged elastic band method (CI-NEB)[29] ((3 × 3) unit cells and two O-Ce-O trilayers). We characterized the transition structures by vibrational analysis. Harmonic vibrational frequencies and normal modes were obtained by diagonalizing the mass weighted force-constant matrix in Cartesian coordinates. A step of ±0.01 Å was set to calculate the force constants.

Keywords: ceria · density functional calculations · nickel · water dissociation · X-ray photoelectron spectroscopy

How to cite: *Angew. Chem. Int. Ed.* **2015**, *54*, 3917–3921
Angew. Chem. **2015**, *127*, 3989–3993

[1] P. A. Thiel, T. E. Madey, *Surf. Sci. Rep.* **1987**, *7*, 211–385.
[2] M. A. Henderson, *Surf. Sci. Rep.* **2002**, *46*, 1–308.
[3] *Catalysis: From Principles to Applications* (Eds.: M. Beller, A. Renken, R. A. van Santen), Wiley-VCH, New York, **2012**.
[4] P. M. Hundt, B. Jiang, M. E. van Reijzen, H. Guo, R. D. Beck, *Science* **2014**, *344*, 504–507.
[5] G. Zhou et al., *Angew. Chem. Int. Ed.* **2010**, *49*, 9680–9684; *Angew. Chem.* **2010**, *122*, 9874–9878.
[6] L. Barrio, A. Kubacka, G. Zhou, M. Estrella, A. Martínez-Arias, J. C. Hanson, M. Fernández-García, J. A. Rodriguez, *J. Phys. Chem. C* **2010**, *114*, 12689–12697.
[7] S. Senanayake, J. Evans, S. Agnoli, L. Barrio, T. Chen, J. Hrbek, J. A. Rodriguez, *Top. Catal.* **2011**, *54*, 34–41.
[8] J. Carrasco, L. Barrio, P. Liu, J. A. Rodriguez, M. V. Ganduglia-Pirovano, *J. Phys. Chem. C* **2013**, *117*, 8241–8250.
[9] Y. Zhou, J. Zhou, *J. Phys. Chem. C* **2012**, *116*, 9544–9549.
[10] A. P. Grosvenor, M. C. Biesinger, R. St. C. Smart, N. S. McIntyre, *Surf. Sci.* **2006**, *600*, 1771–1779.
[11] A. Caballero, J. P. Holgado, V. M. González de La Cruz, S. E. Habas, T. Herranz, M. Salmeron, *Chem. Commun.* **2010**, *46*, 1097–1099.
[12] The VASP site. http://www.vasp.at; version vasp.5.2.12, 11 Nov. **2011**.
[13] Z. Yang, Q. Wang, S. Wei, D. Ma, Q. Sun, *J. Phys. Chem. C* **2010**, *114*, 14891–14899.
[14] D. Fernández-Torre, K. Kósmider, J. Carrasco, M. V. Ganduglia-Pirovano, R. Pérez, *J. Phys. Chem. C* **2012**, *116*, 13584–13593.
[15] M. Molinari, S. C. Parker, D. C. Sayle, M. S. Islam, *J. Phys. Chem. C* **2012**, *116*, 7073–7082.
[16] D. Marrocchelli, B. Yildiz, *J. Phys. Chem. C* **2012**, *116*, 2411–2424.
[17] M. Watkins, T. Trevethan, A. L. Shluger, L. N. Kantorovich, *Phys. Rev. B* **2007**, *76*, 245421.
[18] S. Fuente, M. M. Branda, F. Illas, *Theor. Chem. Acc.* **2012**, *131*, 1190.
[19] D. Fernández-Torre, J. Carrasco, M. V. Ganduglia-Pirovano, R. Pérez, *J. Chem. Phys.* **2014**, *141*, 014703.
[20] a) A. A. Phatak, W. N. Delgass, F. H. Ribeiro, W. F. Schneider, *J. Phys. Chem. C* **2009**, *113*, 7269–7276; b) R. C. Catapan, A. A. M. Oliveira, Y. Chen, D. G. Vlachos, *J. Phys. Chem. C* **2012**, *116*, 20281–20291.
[21] A. A. Gokhale, J. A. Dumesic, M. Mavrikakis, *J. Am. Chem. Soc.* **2008**, *130*, 1402–1414.
[22] J. Nakamura, J. M. Campbell, C. T. Campbell, *J. Chem. Soc. Faraday Trans.* **1990**, *86*, 2725–2734.
[23] D. W. Flaherty, W.-Y. Yu, Z. D. Pozun, G. Henkelman, C. B. Mullins, *J. Catal.* **2011**, *282*, 278–288.
[24] C. T. Campbell, *Nat. Chem.* **2012**, *4*, 597–598.
[25] a) D. Ricci, A. Bongiorno, G. Pacchioni, U. Landman, *Phys. Rev. Lett.* **2006**, *97*, 036106; b) M. Sterrer, T. Risse, U. Martinez Pozzoni, L. Giordano, M. Heyde, H.-P. Rust, G. Pacchioni, H.-J. Freund, *Phys. Rev. Lett.* **2007**, *98*, 096107; c) S. Laursen, S. Linic, *J. Phys. Chem. C* **2009**, *113*, 6689–6693; d) A. Bruix, J. A. Rodriguez, P. J. Ramírez, S. D. Senanayake, J. Evans, J. B. Park, D. Stacchiola, P. Liu, J. Hrbek, F. Illas, *J. Am. Chem. Soc.* **2012**, *134*, 8968–8974; e) A. Bruix et al., *Angew. Chem. Int. Ed.* **2014**, *53*, 10525–10530; *Angew. Chem.* **2014**, *126*, 10693–10698; f) V. Simic-Milosevic, M. Heyde, N. Nilius, T. Konig, H.-P. Rust, M. Sterrer, T. Risse, H.-J. Freund, L. Giordano, G. Pacchioni, *J. Am. Chem. Soc.* **2008**, *130*, 7814–7815.
[26] S. J. Tauster, *Acc. Chem. Res.* **1987**, *20*, 389–394.
[27] A. K. Datye, D. S. Kalakkad, M. H. Yao, D. J. Smith, *J. Catal.* **1995**, *155*, 148–153.
[28] G. E. Murgida, M. V. Ganduglia-Pirovano, *Phys. Rev. Lett.* **2013**, *110*, 246101.
[29] G. Henkelman, B. P. Uberuaga, H. Jónsson, *J. Chem. Phys.* **2000**, *113*, 9901–9904.

Received: November 3, 2014
Revised: December 12, 2014
Published online: February 4, 2015

